Analysis of an Up/Down Power Control Algorithm for the CDMA Reverse Link under Fading *

Lei Song† and Narayan B. Mandayam† and Zoran Gajic
†Wireless Information Network Laboratory (WINLAB)
Department of Electrical & Computer Engineering
Rutgers University
Piscataway, NJ 08854

Abstract: In this paper, we analyze the performance of a CDMA reverse link with an up/down power control algorithm in the presence of fading. We derive a stochastic nonlinear feedback control system model for the power controlled reverse link and study the power control performance based on the nonlinear model using the technique of statistical linearization. We provide a general analysis frame work that allows us to study the effect of mobile speed, power control step size, and fading channel parameters such as correlation coefficient and rate of fading on power control errors. Numerical results show excellent accuracy of our analysis, which can be used to design and optimize the system parameters without going through lengthy simulations. For example, in the presence of shadow fading, it is seen that a power control step size in the range of 0.5 - 1.3 dB is sufficient to keep power control errors near a minimum. In the case of Rayleigh fading, the standard deviation of power control errors grows quickly even at moderate mobile speeds.

Keywords: Power Control, Fading Channel, Nonlinear Control, CDMA.

1 Introduction

Power control is essential in CDMA systems to provide satisfactory quality of service (QoS) and to combat the near-far problem. The QoS for voice is decided by the achieved signal to interference ratio (SIR). On the reverse link, the base station controls the transmit power of the mobile stations so that each user meets its SIR requirement. Power control schemes can be centralized [1, 2] or decentralized [3–5] according to the nature of control. A centralized controller has the information (e.g., all link gains) for each user and it decides control actions for all the users [1,2]. A decentralized controller on the other hand, only utilizes local information to decide the control action for a user (e.g., only uses a user's own link gain and/or SIR to decide its power) [3–5]. A comprehensive survey of power control literature can be found in [6].

*This work is supported in part by the NSF under Grant no. NCR 97-06036. This work was presented in part at the 37th Annual Allerton Conference on Communication, Control, and Computing, Urbana-Champaign, IL, September, 1999.

The study of the performance of the above algorithms (in the literature) often assumes the availability of link information (such as channel gains or SIR values) and its exact exchange between the base station and mobile station. However, in practical systems such as [7,8], the link information is not readily available and the exchange between the base station and mobile station is limited to qualitative information depending on the SIR level achieved. Typically, these are implemented using commands from the base station to the mobile that either increase or decrease the transmit power in (possibly) fixed amounts. As a result, power control is usually done based on (feedback) commands from the base station where the transmit power of the mobile is either increased or decreased. We will refer to this kind of power control as *up/down* power control. In this type of power control, the base station measures the SIR for each user and compares it with a target. A power control bit is then sent to the mobile station on the feedback channel on the forward link in every predetermined epoch referred to as the power control group (PCG) [7]. Thus the transmit power updates at the mobile occur once every PCG based on the one bit feedback to increase or decrease power by a certain amount. Similar limited feedback schemes are also considered in [9–11], however the treatment there does not take into account the coupling between users.

This paper analyzes the reverse link of a CDMA system with this up/down power control algorithm in the presence of fading. Power control with nonlinearity was study in [12] using root locus techniques and describing functions. Stability and convergence properties of a similar up/down power control loop was studied in [13] and [14]. Both works consider nonfading environments. In this paper, we will consider a fading environment. We focus primarily on shadow fading and also extend the analysis to the case of Rayleigh fading and the case with the external interference. We will first model the power controlled reverse link as a stochastic nonlinear feedback control system and then study the its performance using the technique of statistical linearization. Numerical results show excellent accuracy of the approximation. Such an analytical approach can be used to design/optimize the system parameters without going through lengthy simulations. For example, our analysis gives a direct method to evaluate power control stability and errors as a function of mobile speed, power control step size and fading channel parameters such as correlation coefficient and rate of fading.

2 System Model

We consider a CDMA uplink with K users. Considering the observation interval to be infinite, the received signal is given by

$$r(t) = \sum_{k=1}^{K} \sum_{j=-\infty}^{\infty} \sqrt{2p_k(t)} b_{k,j} c_{k,j} s(t - jT_c - \tau_k) e^{j\phi_k} + w(t) \tag{1}$$

- T_c is the chip duration.
- $c_{k,j}$ is the value of the jth chip of the k^{th} user.
- $b_{k,j}$ represents the value of the bit containing the jth chip $c_{k,j}$. It takes on the same value for M successive chips where M is the number of chips in a bit.

- $s(t)$ is the chip waveform, which is assumed to be the same for all users.
- ϕ_k is the phase offset and τ_k is the delay.
- $p_k(t)$ is the received power of user k which is equal to $a_k(t)x_k(t)$.
- $x_k(t)$ is the mobile transmit power and $a_k(t)$ is the link gain.
- $w(t)$ is a zero mean complex Gaussian process with two-sided power spectral density N_0.

We are interested in user 1, whose delay is assumed to be 0. For other users, τ_k is *i.i.d* uniform over $[0, T_c]$. Let $\epsilon_k = \tau_k/T_c$. We will consider a BPSK system with perfect phase estimation[1]. For simplicity, we further assume that the phases of all the users are equal to 0. This implies that all useful information for the signal as well as the interference is contained in the real part of $r(t)$. The bits and chips are +1 and -1 with equal probability. Based on these assumptions, the received signal can be rewritten as

$$\begin{aligned} r(t) &= \sum_{j=-\infty}^{\infty} \sqrt{2p_1} b_{1,j} c_{1,j} s(t - jT_c) + N_t \\ &\quad + \sum_{k=2}^{K} \sum_{j=-\infty}^{\infty} \sqrt{2p_k} b_{k,j} c_{k,j} s(t - jT_c - \epsilon_k T_c), \end{aligned} \tag{2}$$

where $N_t = \mathrm{Re}\{w(t)\}$ is a real Gaussian process with two side PSD $N_0/2$. The receiver is assumed to be a matched filter matched to the spreading waveform $c_1(t)$,

$$c_1(t) = \sum_{j=0}^{M-1} c_{1,j} s(t - jT_c),\ 0 \le t \le MT_c, \tag{3}$$

where we assume $j = 0$ is the first chip in a bit. The decision statistic is

$$D_1 = \int_{-\infty}^{\infty} r(t) c_1(t) dt. \tag{4}$$

Let us define the auto-correlation function of the chip waveform $s(t)$ as

$$R_s(\xi) = \int_{-\infty}^{\infty} s(t) s(t - \xi T_c) dt. \tag{5}$$

Assuming zero inter-chip interference, D_1 in (4) can be written as

$$D_1 = \sqrt{2p_1} M b_1 + \sum_{k=2}^{K} \sum_{m=0}^{M-1} c_{1,m} r_{k,m} + N_k \tag{6}$$

where $r_{k,m} = \sum_{j=-\infty}^{\infty} \sqrt{2p_k} c_{k,j} R_s(j + \epsilon_k - m)$ and $N_k \sim N(0, M\frac{N_0}{2})$, i.e., a zero mean Gaussian random variable with variance $M\frac{N_0}{2}$. Let $I_k = \sum_{m=0}^{M-1} c_{1,m} r_{k,m}$, then

$$E[I_k^2|\epsilon_k] = \sum_{m=0}^{M-1} E(r_{k,m}^2|\epsilon_k) = 2p_k \sum_{m=0}^{M-1} \sum_{j=-\infty}^{\infty} R_s^2(j - m + \epsilon_k) = 2Mp_k \sum_{j=-\infty}^{\infty} R_s^2(j + \epsilon_k). \tag{7}$$

[1]In general, estimation errors in the carrier phase and also the chip waveform timing will contribute to errors in SIR estimation which are not considered here.

Averaging over the distribution of ϵ_k,

$$E[I_k^2[=\int_0^1 E[I_k^2|\epsilon_k]d\epsilon_k = 2Mp_k\sum_{j=-\infty}^{\infty}\int_0^1 R_s^2(j+\epsilon_k)d\epsilon_k = 2Mp_k\sigma_s^2, \tag{8}$$

where $\sigma_s^2=\int_{-\infty}^{\infty}R_s^2(\epsilon)d\epsilon=\int_{-\infty}^{\infty}|\Psi(f)|^4df$. $\Psi(f)$ is the spectrum of the chip pulse waveform. For a rectangular pulse which has a *sinc* spectrum, $\sigma_s=2/3$ [15, 16]. For a *sinc* pulse with rectangular spectrum, $\sigma_s=1$. In practical systems, a raised cosine pulse with excess bandwidth β is commonly used and $\sigma_s^2=1-\beta/4$. Typically, β is close to 0.1 [7] and σ_s is very close to 1. In this paper, we will assume $\sigma_s=1$. Then,

$$E[I_k^2]=2Mp_k \tag{9}$$

Since both the mobile transmit power and the link gain are assumed to be fixed during a Power Control Group (PCG), (which contains multiple chips), the time variable t can be ignored in our analysis. Instead, we can index the above quantities by PCGs and derive a discrete model. Then, in the nth PCG, D_1 has mean $\sqrt{2p_1(n)}M$ and variance $(2\sum_{k=2}^K p_k(n)+N_0/2)M$. We assume that the SIR for user 1 can be estimated perfectly by the base station[2]. The SIR for user 1 can be written in discrete form as

$$\gamma_1(n)=\frac{2p_1(n)M}{2\sum_{k=2}^K p_k(n)+N_0/2}=\frac{2a_1(n)x_1(n)M}{2\sum_{k=2}^K p_k(n)+N_0/2}, \tag{10}$$

where n is the PCG iteration index. Note that while (10) is derived under the assumption that the phase $\phi_k=0$, for all k, it is easy to derive an appropriate expression as in (10) even when the phases are random[3].

To facilitate a tractable analysis, we will assume that $p_k(n)$ is controlled around the target p_k^* and replace $\sum_{k=2}^K p_k(n)$ by $\sum_{k=2}^K p_k^*$. In [13], we showed that $p_k(n)$ will converge to a neighborhood of p_k^* for feasible systems with constant link gains. Essentially, we assume that the sum of a large number of interferers is relatively constant during a frame. Note that we do not need to estimate p_k^*. We will show that our proposed analytical results are valid as long as the sum remains close to a constant. Such treatment of $p_k(n)$ is also consistent with the results in [19] as well as experimental measurements of [20, 21]. This approximation removes the correlation in the received power from interferers and simplifies the problem. Finally, equation (10) is reduced to

$$\gamma_1(n)=\frac{2a_1(n)x_1(n)M}{2\sum_{k=2}^K p_k^*+N_0/2} \tag{11}$$

We will use the capital letters to denote values in dB. In dB, equation (11) can be written as

$$\Gamma_1(n)=A_1(n)+X_1(n)-I \tag{12}$$

[2]In general, errors in SIR estimation increase the standard deviation of the power control errors. For the effect of SIR measurements on power control, we refer the reader to [17] and for results on SIR estimation in CDMA systems, we refer the reader to [18].

[3]For random phases, Equation (4) becomes $D_1 = Re[\int_{-\infty}^{\infty}r(t)c_1(t)dt] = \sqrt{2p_1}Mb_1 + \sum_{k=2}^K\sum_{m=0}^{M-1}c_{1,m}r_{k,m}cos(\phi_k)+N_k$, where $\phi_k\sim U[0,2\pi)$. Equations (8) - (10) can be modified accordingly by averaging over the distribution of the phases ϕ_k. The resulting SIR equation is similar to Equation (10) and the analysis in the paper will apply. This point will be further verified in the numerical results section

where I is a constant given by

$$I = 10 \log \frac{2 \sum_{k=2}^{K} p_k^* + N_0/2}{2M} \tag{13}$$

At the base station, $\gamma_1(n)$ is compared with a target γ_1^{tar} to decide to either raise or lower the received power for user 1. Since M is a constant, without loss of generality, we can normalize γ_i^{tar} by M. Thus, in the remainder of the paper, γ_i^{tar} will denote γ_i^{tar}/M. Equivalently, we can compare Γ_1 with Γ_1^{tar} since log is a monotonic function. Note that for convenience, both Γ_i and Γ_i^{tar} can be normalized too. If $\Gamma_1 < \Gamma_1^{tar}$, the base station will command the mobile to reduce its power by d dB; otherwise to increase its power by d dB. In a practical system such as [7], γ_1^{tar} is adapted slowly by an outer loop to guarantee a certain QoS such as FER. The adaptation is usually very slow, so that when we focus on the fast inner loop, γ_1^{tar} can be treated as a fixed reference. Finally, we can write the state equation for the up/down power control algorithm as a nonlinear difference equation:

$$X(n+1) = X(n) + d\Psi(\Gamma^{tar} + I - X(n) - A(n)) \tag{14}$$

where the nonlinear term Ψ is defined as:

$$\Psi(x) = \begin{cases} 1 & \text{if } \; x \geq 0 \\ -1 & \text{if } \; \text{otherwise} \end{cases} \tag{15}$$

Since user 1 is the user being considered, we drop the subscript 1 for simplicity. The system of equations (14) and (15) can be represented via the block diagram of a nonlinear feedback control system as shown in Figure 1. Since the adjustment at a PCG depends on the SIR measurement of the previous PCG, a PCG power control delay is introduced in the feedback portion of Figure 1. Note that the channel gain $A(n)$ (interference I as well, if I is not constant) needs to be delayed for 1 PCG as well. This delay is represented by a delay component in Figure 1. The input to the

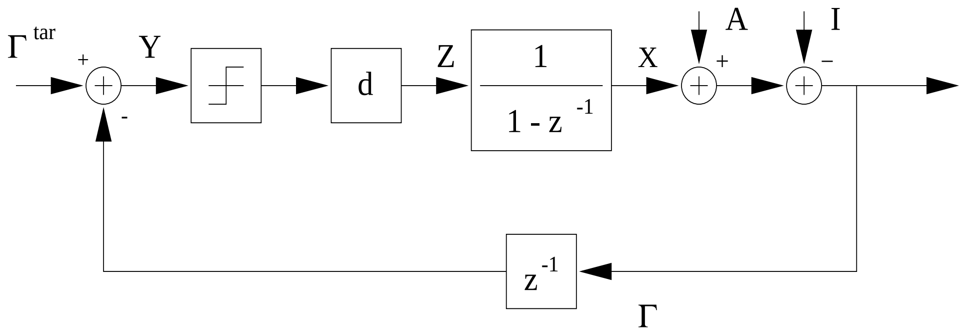

Figure 1: Block diagram for the up/down power control algorithm

nonlinear system is the link gain sequence $\{A(n)\}$. The link gain depends on the propagation loss due to the distance, shadowing by buildings and other objects as well as rapid Rayleigh fading. The propagation is usually compensated by the open loop adjustment of an Automatic Gain Control unit (AGC). The rapid variation due to Rayleigh fading may be considered to be averaged out in a

PCG. This leaves shadowing as the main factor in deciding the characteristics of the channel gain sequence used as the input to system (14). We first consider only the case of shadow fading and later show in sections 5 and 6 how the analytical techniques here can be extended to the case of Rayleigh fading and the case with the presence of external interference. Note that in equations (11) - (13), we have treated the AWGN noise $N(t)$ only through its power spectral density $N_0/2$. This is under the assumption that during a PCG several samples of the received signal are averaged to obtain the SIR. Later, in Section 6, we will consider the case with the presence of additive external interference which can not be averaged out. For shadow fading, empirical studies have shown that $a(n)$ follows a log-normal distribution [19,22]. This implies $A(n)$ is Gaussian. A simple and realistic model of $A(n)$ is a Gaussian process with the correlation given as (see [22] pp. 90):

$$R_A(n) = \sigma_A^2 \xi^{(vT/D)|n|} \tag{16}$$

where

- ξ is the correlation between two points separated by a spatial distance of D.
- T is the sampling period which is the length of a PCG for the system (14).
- v is the speed of the mobile. vT gives the distance covered by the mobile in a sample interval.

Different channels are characterized by different values of ξ, D and v. Some experimental values for different environments can be found in the experimental studies of [23, 24]. Also note that in (14), we can combine A with I and Γ by defining

$$B(n) = -A(n-1) + I + \Gamma^{tar}. \tag{17}$$

Note that $B(n)$ is still a Gaussian process with the same covariance as $A(n)$. The state equation is simplified as:

$$X(n+1) = X(n) + d\Psi(B(n+1) - X(n))) \tag{18}$$

3 Analysis via statistical linearization

To evaluate the performance of the power control algorithm, we are interested in finding the distribution of the SIR error $Y(n) = \Gamma^{tar} - \Gamma(n-1)$. A narrow *pdf* centered at 0 implies tight power control. However, to find the *pdf* of $Y(n)$ from Equation (14) is not simple. The *pdf* can be found using the method of Markov Process outlined in ([25], Chapter 1). A brief description of the method is given as follows.

This method is based on Markov theory which states that the *pdf* of the response of a dynamic system to white noise excitation satisfies the partial difference equation called the Fokker-Planck-Kolmogorov (PFK) equation [25]. This method is the utmost method in providing an analytical nonlocal solution for a general nonlinear system. However, solving the PFK equation is very difficult. Analytical solutions are possible only for some limited cases. In our power control problem, the input is correlated because otherwise power control should not be even attempted due to its inherent delay. We can approximate $A(n)$ by passing white-noise through a linear filter. This will increase the order of the system and leave the system very difficult to solve. As an alternative, local methods such as perturbation methods and statistical linearization may be used [25, 26]. Perturbation methods are not feasible for this power control problem due to the discontinuity of $\Psi(\,)$ at 0. In this paper, we will analyze the system through the technique of statistical linearization.

The statistical linearization approach [27] is based on the concept of approximating the solution to a nonlinear random system by that obtained from an "equivalent" linear system. The equivalent linear system is obtained by replacing the nonlinear component with a linear one which minimizes a certain objective function such as mean square error within a certain class of linear approximators. The best linear approximation depends on the statistics of the input signal to the nonlinear component. On the other hand, the statistics of the input signal can also be found by solving the equivalent linear system once the best linear approximator is decided. Thus, we can set up an equation for the input signal statistics.

An inherent difficulty of this approach is that this equation not only contains the first and second moments but higher moments as well and some time even the entire *pdf* is needed. To overcome this difficulty, some hypothesis is usually introduced concerning the nonlinear input signal *pdf*. And the functional equation is simplified into an algebraic or transcendental equation of some parameters such as low order moments.

Let us consider a feedback system consisting of a nonlinear memoryless component and a linear component. If the input signal is a Gaussian random process and the nonlinearity is a lagless odd function, then it can be shown ([26], section 4.6) that the system response is approximately Gaussian if the frequency band of the external signal does not coincide with the frequency band of the linear component. Since the power adaptation in (14) is faster than the channel variation (i.e., the external signal), we shall approximate $X(n)$ as Gaussian. Consequently, $Y(n)$ is Gaussian as well. This assumption is also consistent with the classical treatment in [19].

We will further assume that $Y(n)$ has zero mean. An intuitive argument is given as follows. Suppose $Y(n)$ is a Gaussian process with a positive mean. Then, $Prob\{Y(n) > 0\} - Prob\{Y(n) \leq 0\} > 0$. The output of the hardlimter $Z(n)$ in Figure 1 is a sequence of $+d$'s and $-d$'s, with $Prob\{Z(n) = d\} = Prob\{Y(n) > 0\}$ and $Prob\{Z(n) = -d\} = Prob\{Y(n) \leq 0\}$. Then,

$$E\{Z(n)\} = d\ Prob\{Z(n) = d\} - d\ Prob\{Z(n) = -d\} = d\Delta,$$

where $\Delta = Prob\{Y(n) > 0\} - Prob\{Y(n) \leq 0\} > 0$. Note that from Figure 1,

$$X(n) = X(n-1) + Z(n),$$

Then,

$$E\{X(n)\} = E\{X(n-1)\} + E\{Z(n)\} = E\{X(n-1)\} + d\Delta = E\{X(0)\} + nd\Delta.$$

Thus, the mean of $X(n)$ increases linearly with the PCG index n. Consider $\Gamma(n) = X(n)+A(n)-I$. Note that $A(n)$ has a constant mean. Therefore, the mean of $\Gamma(n)$, increases linearly with the index n. Further, since $Y(n) = \Gamma^{tar} - \Gamma(n-1)$, $Y(n)$ must have a mean decreasing linearly with the PCG index n (since Γ^{tar} is fixed). Therefore, we note that as $n \to \infty$, $E\{Y(n)\} \to -\infty$. This contradicts the assumption that $Y(n)$ has a positive mean. Similarly, it can be argued that $Y(n)$ can not have a negative mean either. Thus, the mean of the power control error sequence $Y(n)$ must be zero.

Now we only need to focus on finding the variance of $Y(n)$ by statistical linearization. The simplest linear approximation is to replace a nonlinear component $f(x)$ with a constant gain. The best approximator K^* minimizes an objective function such as $E\{(Kx - f(x))^2\}$. This simple approximation was shown to generate reasonably good results for continuous nonlinear systems in [25, 26]. However, we find that for the discrete nonlinear system such as in (14), this simple linearization drastically underestimates the variance of $Y(n)$. Instead, we propose to approximate $d\Psi(\ )$ with a constant gain K and an uncorrelated random noise with the restriction that the equivalent term results in the same mean and variance as the original nonlinear term. In other words, we want to approximate the output of $Z = d\Psi(Y)$ with $\hat{Z} = KY + W$ for some constant gain K and white noise W with a constraint that Z and $\hat{Z}$ have the same mean and variance. This approximation is shown in Figure 2. Within this class of linear approximators, the optimal one is defined as the one that minimizes the MSE $E\{(Z - KY)^2\}$. Note that Z being zero mean implies that W has zero mean as well.

Let $Y \sim N(0, \sigma_Y^2)$. Assuming σ_Y is known, we shall find the optimal K and σ_W as functions of σ_Y. To find K^*, we proceed as follows:

$$\begin{aligned} E\{(Z - KY)^2\} &= E\{Z^2\} + K^2 E\{Y^2\} - 2KE\{YZ\} \\ &= 1 + K^2\sigma_Y^2 - 2KE\{YZ\} \end{aligned} \tag{19}$$

Taking the partial derivative,

$$\frac{\partial E\{(Z - KY)^2\}}{\partial K}\Big|_{K=K^*} = 2K^*\sigma_Y^2 - 2E\{YZ\} = 0 \tag{20}$$

This yields

$$K^* = \frac{E\{YZ\}}{\sigma_Y^2} = \frac{\sqrt{\frac{2}{\pi}}d}{\sigma_Y^2} \tag{21}$$

The variance of W can be found using the constraint that Z and $\hat{Z}$ have the same variance.

$$E\{\hat{Z}^2\} = (K^*)^2 E\{Y^2\} + E\{W^2\} = E\{Z^2\}, \tag{22}$$

which implies

$$E\{W^2\} = (1 - \frac{2}{\pi})d^2 \tag{23}$$

Replacing $d\Psi(Y)$ with $K^*Y + W$, we have the equivalent linear system shown in Figure 2. We use two approaches to find σ_Y in terms of K^*, namely (1) The spectrum integration approach and (2) The Lyapunov equation approach.

3.1 Spectrum Integration Approach

The transfer function from B to X is

$$H_{B,X}(e^{-jw}) = \frac{e^{-jw}}{1 - (1 - K^*)e^{-jw}} \tag{24}$$

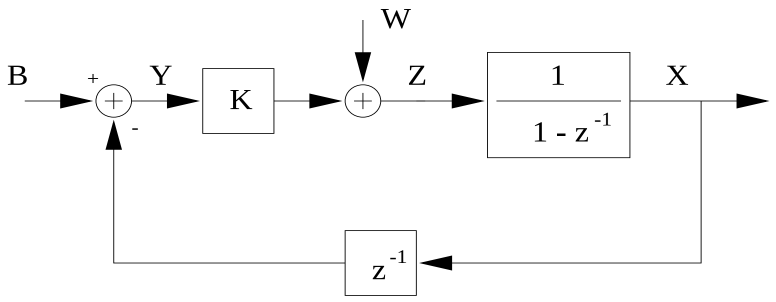

Figure 2: Block diagram for the equivalent linear system

and thus the transfer function between B and Y is

$$H_{B,Y}(e^{-jw}) = 1 - H_{B,X}(e^{-jw}) = \frac{1 - e^{-jw}}{1 - (1 - K^*)e^{-jw}} \tag{25}$$

The transfer function from W to Y is

$$H_{W,Y} = \frac{-1}{1 - K^* e^{-jw}} \tag{26}$$

Thus the variance of Y is given as

$$E\{Y^2\} = \frac{1}{2\pi} \int_{-\pi}^{\pi} |H_{B,Y}(e^{-jw})|^2 S_B(e^{-jw}) dw + \sigma_W^2 \int_{-\pi}^{\pi} |H_{W,Y}(e^{-jw})|^2 dw \tag{27}$$

where $S_B(e^{-jw})$ is the spectrum of B and is given by

$$S_B(e^{-jw}) = \frac{(1 - \xi^{2vT/D})^2}{|1 - \xi^{2vT/D} e^{-jw}|^2} \tag{28}$$

The first term on the right-had side of equation (27) is the contribution from channel variation B and the second term from noise input W. The variance of Y can be solved numerically once the spectrum of B is known. The solution always exists due to the following reason. For a fixed step size d, the variance of W is independent of K. So the second term is a constant. The first term, which is the variance contribution from B does depend on K^*. Note that $H_{B,Y}$ has one zero at e^{jw} and a pole at $\frac{1}{1-K^*} e^{jw}$. It will suppress the low frequency component and may magnify the high frequency component, depending on the value of K^*. If K^* is approaching zero, the first term approaches the variance of B. If K is approaching 2, while the system is still stable, the high frequency part of $\Delta B(k) = B(k) - B(k-1)$ is significantly magnified, and results in large variance of $Y(k)$. On the other hand, the curve of $\sigma_Y^2 = \frac{\sqrt{\frac{2}{\pi}} d}{K^*}$ is monotonically decreasing from infinity for $K^* = 0$ to $\frac{\sqrt{2/\pi}}{2}$ for $K^* = 2$. Since both curves are continuous, a solution satisfying (21) and (27) must exist. The solution can be found by numerically integrating (27) for each K^* and then finding the intersection with the curve $\sigma_Y^2 = \frac{\sqrt{\frac{2}{\pi}} d}{K^*}$.

3.2 Lyapunov Equation Approach

The spectrum integration method works for a general fading process which is Gaussian. If the fading can be further modeled as a Gaussian white noise process filtered by a low pass filter, the power control error variance can be obtained more efficiently using the Lyapunov equation [28].

Consider the model suggested by Gudmundson [24],

$$B(k+1) = \alpha B(k) + (1-\alpha)U(k)$$

where α is a parameter that controls the spatial decorrelation of the shadowing and $U(k)$ is a zero-mean Gaussian random process. The spectrum of $B(k)$ is exponential. A more general model for a random process with exponential spectrum is

$$B(k+1) = \alpha B(k) + \beta U(k).$$

The variance of power control error Y can be found by considering $U(k)$ and $W(k)$ as two inputs, both of which are zero-mean Gaussian random process. Starting from an initial guess of the value of K^*, the state space equation can be written as:

$$\begin{bmatrix} X(k) \\ X(k+1) \end{bmatrix} = \begin{bmatrix} 0 & 1 \\ -\alpha(1-K^*) & 1-K^*+\alpha \end{bmatrix} \begin{bmatrix} X(k-1) \\ X(k) \end{bmatrix} + \begin{bmatrix} 0 & 0 & 0 \\ -K^*\beta & K^*\alpha & K^* \end{bmatrix} \begin{bmatrix} U(k) \\ W(k-1) \\ W(k) \end{bmatrix}$$

and the output equation is

$$Y(k) = [\frac{1}{K^*} \quad -\frac{1}{K^*}] \begin{bmatrix} X(k) \\ X(k+1) \end{bmatrix} + [0 \;\; 0 \;\; -K^*] \begin{bmatrix} U(k) \\ W(k-1) \\ W(k) \end{bmatrix} \tag{29}$$

Let V_X be the covariance of state variable $\underline{X}(k) = \begin{bmatrix} X(k-1) \\ X(k) \end{bmatrix}$,

$$V_X = \begin{bmatrix} \sigma_X^2 & R_X(1) \\ R_X(1) & \sigma_X^2 \end{bmatrix} \tag{30}$$

and V_I be the covariance of the input $\begin{bmatrix} U(k) \\ W(k-1) \\ W(k) \end{bmatrix}$, i.e.,

$$V_I = \begin{bmatrix} \sigma_U^2 & 0 & 0 \\ 0 & \sigma_W^2 & 0 \\ 0 & 0 & \sigma_W^2 \end{bmatrix} \tag{31}$$

For simplicity, let us denote

$$\begin{aligned} a &= -\alpha(1-K^*) \\ b &= 1-K^*+\alpha \end{aligned} \tag{32}$$

and define a matrix H

$$H = \begin{bmatrix} 0 & 1 \\ a & b \end{bmatrix}.$$

Let us define

$$G = \begin{bmatrix} 0 & 0 & 0 \\ -K^*\beta & K^*\alpha & K^* \end{bmatrix}.$$

The covariance matrix of $\underline{X}$ satisfies the following equation.

$$V_X = HV_XH^T + GV_IG^T \tag{33}$$

This is an algebraic Lyapunov equation [28]. The solution is given as

$$\sigma_X^2 = \frac{(1-a)(K^{*2}\beta^2\sigma_U^2 + K^{*2}\alpha^2\sigma_W^2 + K^{*2}\sigma_W^2)}{1-a^2-b^2-ab^2+a^3} \tag{34}$$

and

$$R_X(1) = \frac{b}{1-a}\sigma_X^2 \tag{35}$$

The variance of Y can be found as

$$\begin{aligned} \sigma_Y^2 &= \frac{2}{K^{*2}}(\sigma_X^2 - R_X(1)) + \sigma_W^2 \\ &= \frac{2(1-a-b)}{K^{*2}(1-a)}\sigma_X^2 + \sigma_W^2 \end{aligned} \tag{36}$$

The above equation can be rewritten as a fifth order polynomial equation for σ_Y. Then σ_Y can be solved iteratively using equations (36) and (21) where we successively iterate between the values of K^* and σ_Y^2.

4 Numerical Results

In this section, we present numerical results on the analysis of the up/down power control algorithm in the presence of log-normal shadow fading. We consider the reverse link of a single cell system with N users each employing the up/down power control algorithm. In order to validate the analysis, we perform simulations that include the power control loop implementations for all the users and also the interaction of these users as interference to each other. The simulation model is shown in Figure 3. Note that in Figure 3, the nonlinear feedback control system that reflects the power control loop for each user is also excited by the transmit power outputs that result from the power control loops of the other users. The shadow fading is introduced into the model for the ith user via the sequence $A_i(n)$, which is a Gaussian process with the correlation given in equation (16). The mobile speed v, the correlation parameter ξ and σ_A^2 are used to parameterize the correlation process in the numerical results described here.

Note that in our analysis, the only assumption on the interference is that it remains close to constant. The simplifying assumption of treating the sum of interferers as a constant (see equations (11) - (13)) is done only to make the analysis more tractable. To compare the analytical results with simulations, in the simulation model in Figure 3, we do not assume the total interference is a constant. Instead, it is generated through actual power control of each user. In other words, we do not replace $\Sigma_{k\neq i} p_k(n)$ with $\Sigma_{k\neq i} p^*_k(n)$. The simulations takes into account the effect of the correlation in the received power from interfering users. Thus the inaccuracy of the analysis are not only due to the statistical linearization but also includes the error due to interference model simplification.

The function $f(\ )$ converts dbW to W and is defined as $f(x) = 10^{x/10}$. The function $g(\ )$ calculates $I_i(n)$ based on the interference from other users and it is defined as $g(x) = 10 \log \frac{2x+N_0/2}{2}$. For the 2-user simulation, the speed of the other mobile is 100 kmph. For the 16-user simulation, the speeds for other mobiles are uniformly distributed from 1 to 300 kmph. In the results shown, the SIR targets are the same for all the users and they are chosen such that the total received power is 9 dB over the noise floor $N_0/2$, i.e., $\sum_{i=1}^{N} \gamma_i^{tar} = 0.89$. Thus, for the 2-user case, $\Gamma_i^{tar} = 10\log(0.89/2)$ for both users. For the 16-user case, $\Gamma_i^{tar} = 10\log(0.89/16)$ for all 16 users[4]. In the simulation, the noise floor $N_0/2$ is set at -100 dBW. The initial values of the received power $X_i(0)$ is set at -95 dBW for all users. The random inputs that drive the simulation model are the fading sequences $A_i(0), ...A_i(n), ...$ for $i = 1, ..., N$. Note that the power control loops for all the users are interconnected through the interference, which is calculated from the sum of the received power from all other users and the noise using the function $g(\ )$.

The analytical results are compared with simulations as follows. The power control error standard deviation σ_Y v.s speed v is plotted in Figure 4. To see the effect of channel correlation, the plot of σ_Y vs ξ is shown in Figure 5. To validate our analysis, simulation results as well as analytical results using spectrum integration and Lyapunov equation are plotted in all figures. The solid curves are the simulation results for different number of users. Note that the constant values of p_k do not affect the variance σ_Y in the analysis. The dash-dotted curve is the analytical result using spectrum integration and the dashed curve is the analytical result obtained by solving the Lyapunov equations.

We state in the following some observations regarding the results:

- Compared with 1-user simulation results, the analytical approach slightly underestimates at low speeds and overestimates at high speeds. Overall, the analytical results match the simulation results results very well. This shows that our statistical linearization approach is valid and accurate.

- For the 1-user case, the only interference is the constant noise floor. The worst case is the 2-user system, where the interference from a single user fluctuates enough to not be a constant as we have assumed in our analysis. Simulation results for the 1-user system match that of the 16-user system. This suggests that the approximation in (11) is valid when there are many users in a system and no dominant ones.

- The analytical results obtained through spectrum integration match that obtained by solving

[4] The purpose of comparing a 2-user case with a 16-user case is to show how the approximation in (11) performs for systems with different number of users. We require that both systems have the same received power, i.e., the same loading, which results in different Γ_i^{tar}.

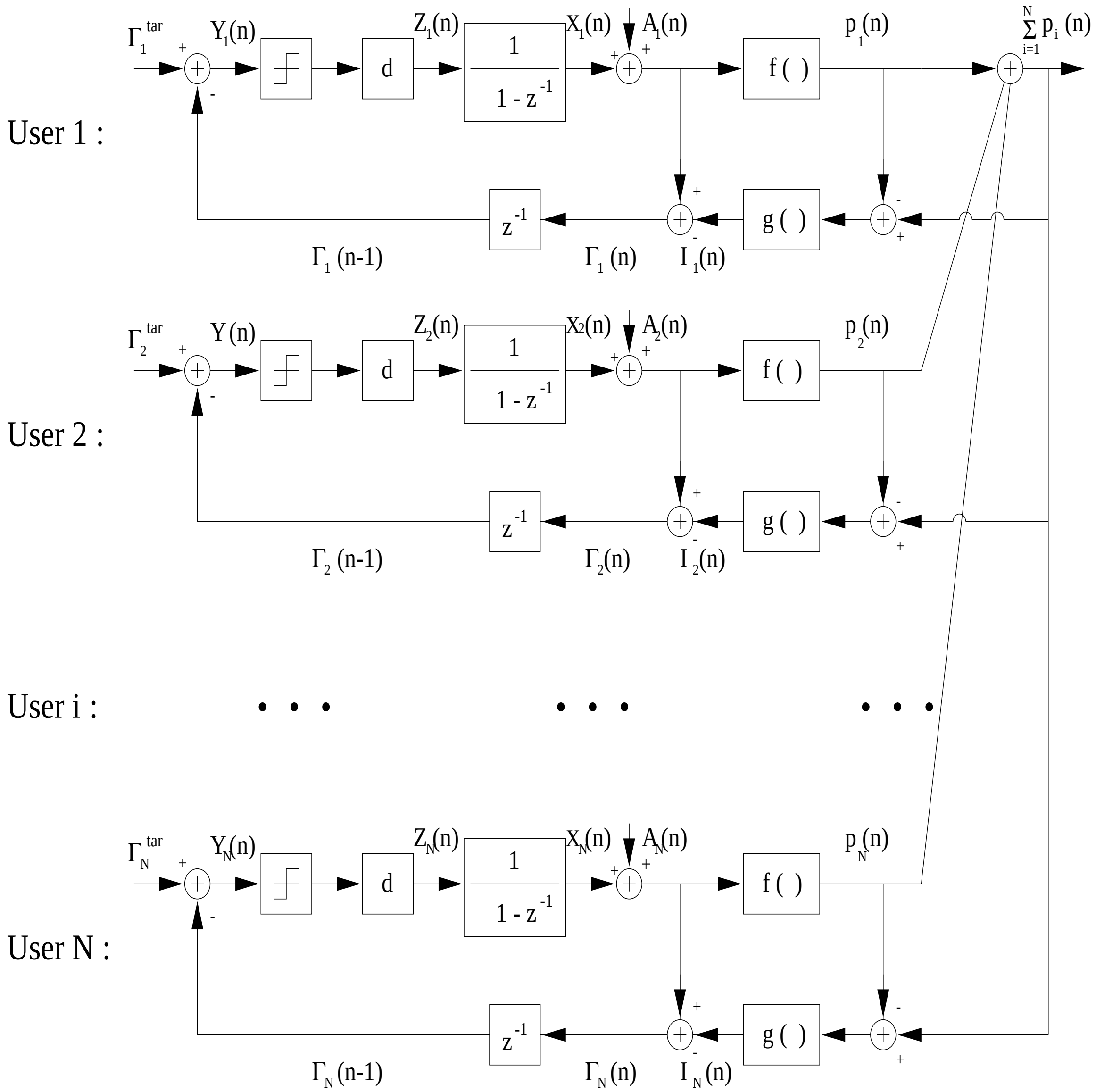

Figure 3: Simulation model

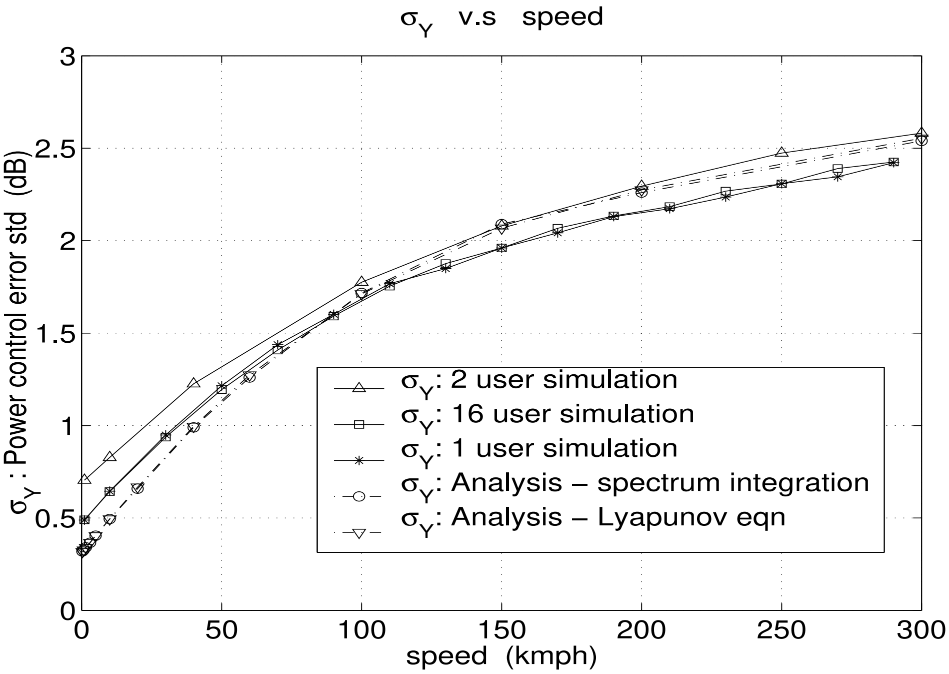

Figure 4: σ_Y v.s v ($d = 0.5$ dB, $D = 1$ m, $\xi = 0.1$, $T = 1.25$ ms, $\sigma_A = 3$ dB.)

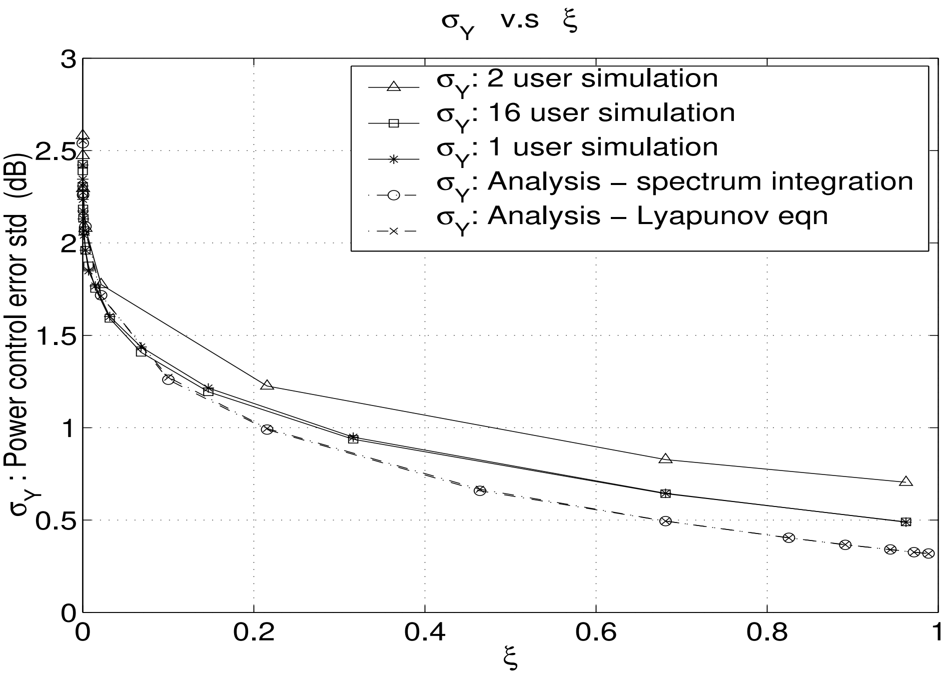

Figure 5: σ_Y v.s. correlation ξ ($d = 0.5$ dB, $D = 1$ m, $v = 60$ kmph, $T = 1.25$ ms, $\sigma_A = 3$ dB.)

the Lyapunov equation. The small variation is caused primarily by the inaccuracy in numerical integration of the spectrum. The Lyapunov method gives a polynomial equation which can be solved very conveniently. In most of the later results in the section, only the Lyapunov method is used to obtain the analytical results.

- At a very slow speed, $\sigma_Y \approx 0.25$ dB. Note that for a non-fading channel, the power adjustment will be alternating up and down adjustments. For $d = 0.5$ dB, it results in a variance of 0.25 dB. This implies that the variance is primarily caused by the power control algorithm. Therefore, a smaller step size is more beneficial at very low speeds.

- For high speeds, σ_Y is primarily caused by the channel variation. Both the analytical method and our simulations show that $\sigma_Y \to 3.16$ dB as the speed approaches infinity. Note that the value of 3.16 dB is in the ball park of the channel variance which is 3 dB.

The second test is to see how the power control algorithm works with different step size d. Assuming the same parameters for the channel and a mobile speed of 60 kmph, σ_Y is plotted in Figure 6. In the simulation, we assume there are 16 users in the system. We state below some observations regarding the results:

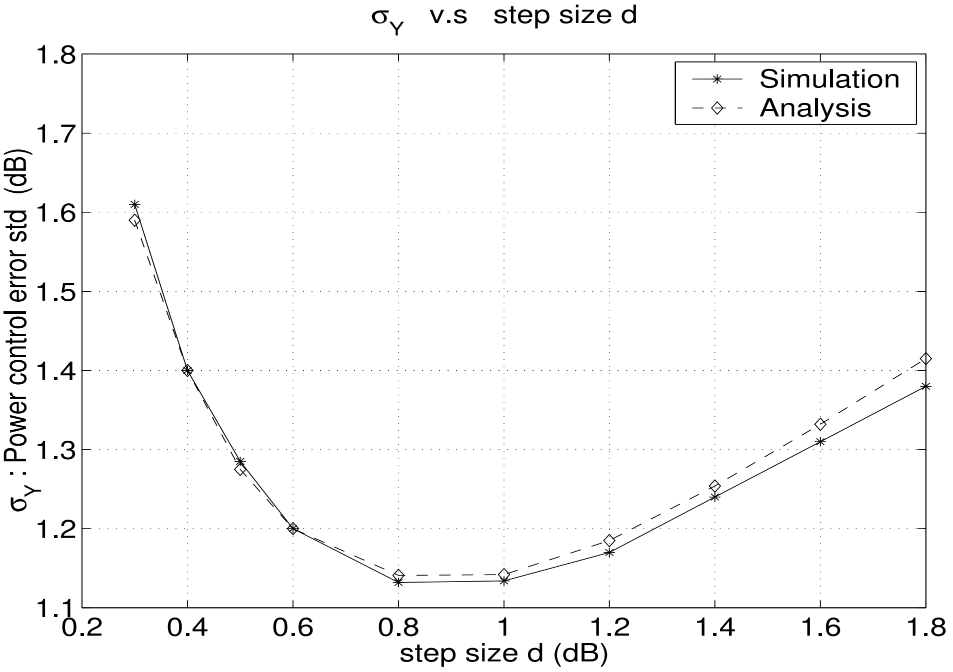

Figure 6: σ_Y v.s. d ($v = 60$ kmph, $D = 1$ m, $\xi = 0.1$, $T = 1.25$ ms, $\sigma_A = 3$ dB.)

- If a step size is too small, it may not be efficient to compensate the channel fading; On the other hand, if the step size is too large, it may overly compensate and thus introduce extra variance in power control error. The optimal step size in this example is about 0.8 dB.

- Using the assumed parameters, the performance seems to be not very sensitive to the step size. In the range between 0.5 dB and 1.3 dB, the performance in terms of the power control variance σ_Y^2 is quite close to the optimum value of 1.12 dB for this example.

An interesting question is to find the optimal step size d for users with different speeds. Simulations are typically very time consuming and practically only picks the best one from a set of candidate step sizes. The analytical approach using Lyapunov equation is very efficient. The optimal step size for different speeds are plotted in Figure 7. An important observation is that the optimal step size depends on the mobile speed, or the channel correlation factor. We can see that at low speeds, a smaller step size should be used since the fading is slow. When the speed increases, channel variation increases and the optimal step size increases. It can be shown by our analysis (not shown here) that if the speed is too high, the optimal step size decreases again. We find that the optimal step size reaches the maximum at speed a close to 300 kmph.

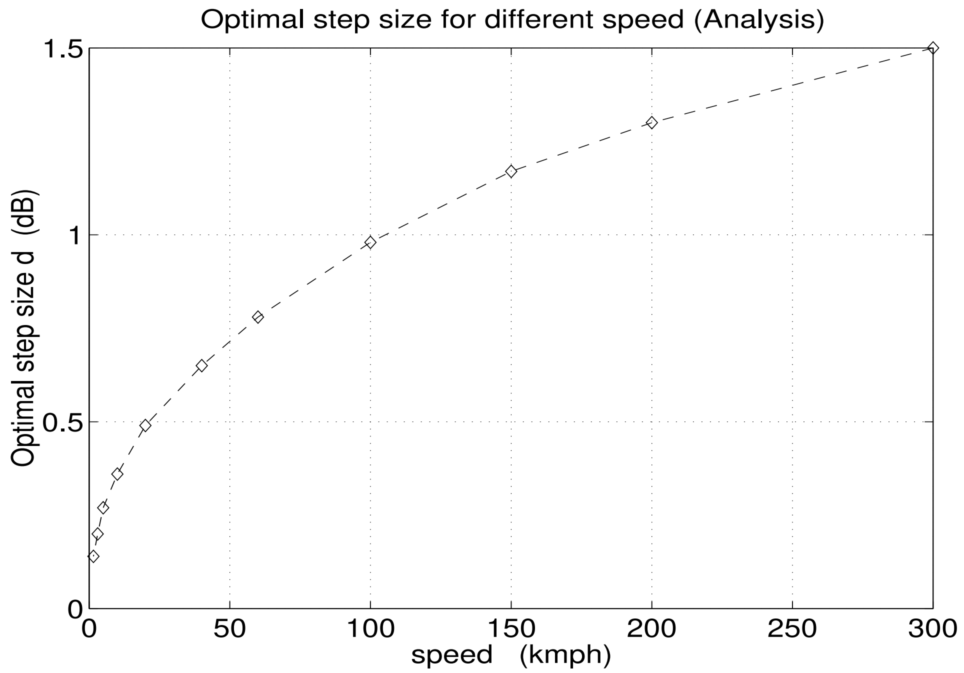

Figure 7: Optimal step size d v.s. speed v ($D = 1$ m, $\xi = 0.1$, $T = 1.25$ ms, $\sigma_A = 3$ dB.)

In the above simulations, we have assumed that all the users have phases that are identically zero. We now consider the effect of non-zero phases on the performance of the power control algorithm (see Footnote 3). Note that the analysis for this case remains unchanged since we assume that the total interference is relatively constant (see equation 11). The effect of having a non-zero phase ϕ_k is to replace p_k^* by $p_k^* cos^2 \phi_k$ in the SIR expression in equation (11). Even though I in equation (13) has a different value now, this only affects the mean of B in equation (17). The variance and auto-correlation of B are thus unaffected and as has already been shown this does not change the variance of the power control error. For simulating the effect of random phases, we modify the simulation model in Figure 3 to include the effect by scaling all powers $p_k(n)$ with $cos^2\phi_k$ where $\phi_k \sim U[0, 2\pi]$. The results are shown in Figure 8 where we have plotted the analysis curve as well as 2 and 16 user simulation results. We observe that the simulation results match well the analysis results and also seem to suggest that the unequal phases do not affect much the performance of the up/down power control algorithm.

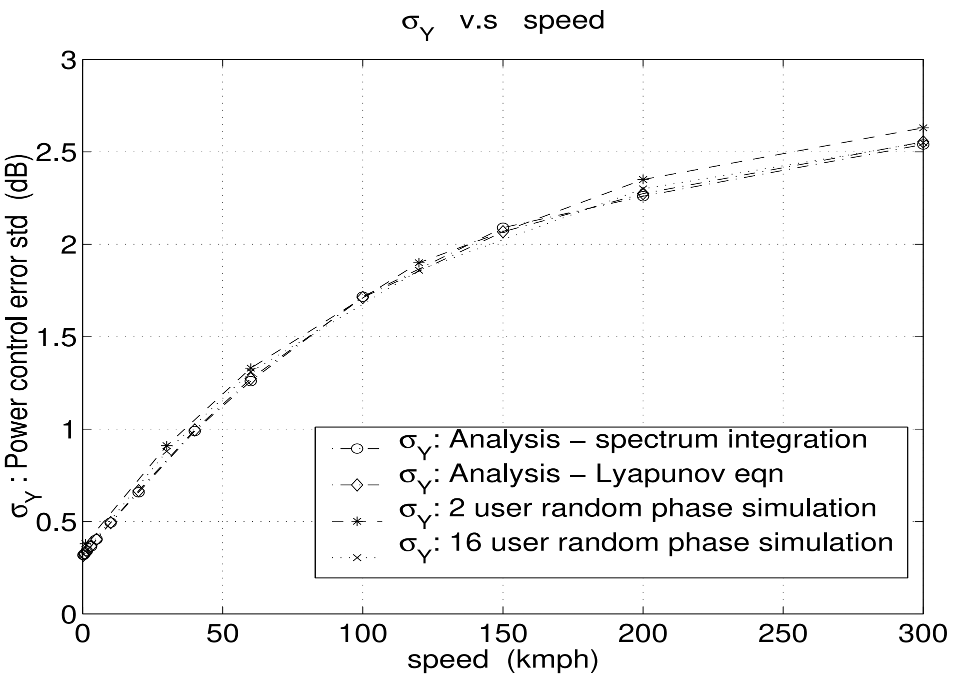

Figure 8: σ_Y v.s v ($d = 0.5$ dB, $D = 1$ m, $\xi = 0.1$, $T = 1.25$ ms, $\sigma_A = 3$ dB, $\phi_k \sim U[0, 2\pi]$.)

5 Application of statistical linearization to Rayleigh fading channels

Thus far we have primarily focused on shadow fading, which has a log-normal distribution. However, if the up/down power adjustment is done at a high frequency, it is also capable of combating fast fading to some degree [11, 29]. The practical issue is one of how quickly the system can issue the feedback commands to the mobile. It is meaningful to know if the statistical linearization technique can apply to other fading channels such as those suggested by ITU in [29].

A general answer is that this technique may apply if we have a certain knowledge of the fading channel statistics to obtain a reasonable initial guess of the distribution of the input to the hard-limiter (i.e., power control error). It is known that in fast fading conditions, such as in Rayleigh fading channels, the power control error may still have a distribution close to log-normal [20]. We will use this assumption from [20] and consider the analysis of the up/down power control algorithm through the statistical linearization technique. Numerical results show that this linearization technique for analysis works well in fast fading channels as well. We will present a numerical example to demonstrate the accuracy of the techniques.

Let us consider a one-path Rayleigh fading channel. The state equation (18) is once again given as:

$$X(n+1) = X(n) + d\Psi(B(n+1) - X(n)),$$

where

$$B(n+1) = -A(n) + I + \Gamma^{tar}$$

The link gain $A(n)$ is obtained in this case by taking the logarithm of the Rayleigh fading process $a(n)$ instead of a shadow fading process. The interference I is assumed to be a constant as in the case of shadow fading. The power control error variance σ_Y can be calculated as follows. For a variance σ_Y, the optimal K^* is given by equation (21) as $K^* = \frac{\sqrt{\frac{2}{\pi}}d}{\sigma_Y^2}$. For a given K^*, the variance σ_Y can found by equation (27). However, note that we require the power spectrum $S_B(e^{-jw})$ of the process $B(n)$. We can obtain the spectrum numerically from the sequence $B(n)$ via for instance, the Blackman-Tukey spectral estimation algorithm [30]. The spectrum only depends on the channel fading process $A(n)$ and can be estimated numerically prior to the calculation of the variance σ_Y. Thus, given an initial guess of K^*, the power control error σ_Y can be calculated iteratively using equations (21) and (27).

In our example, the channel is simulated using a filtered Gaussian noise model [22]. The power control step size d is chosen to be 1 dB. In Figure 9, σ_Y by analysis is compared with that obtained by simulation for a 16-user system. The speeds are ranging from 0.3 kmph to 150 kmph. We observe very good accuracy between the analysis and simulations. The results show that the up/down power control is effective only when then mobile speed is slow.

6 Application of statistical linearization in the presence of external interference

In order to test the versatility of the analysis technique, we also performed tests to see how the power control works in the presence of external interference. Such external interference in a CDMA system may arise from surrounding cells or other systems such as AMPS or TDMA [31]. A detailed explanation of possible sources of external interference can be found in Chapter 7 of [32]. Let $\eta^2(n)$ be the external interference power received at the base station receiver in the nth PCG. The SIR for user 1 in the nth PCG is then given as:

$$\gamma_1(n) = \frac{2p_1(n)}{2\sum_{k=2}^{K} p_k^* + \eta^2(n) + N_0/2} \tag{37}$$

In general, it is difficult to model the process $\eta^2(n)$ because its statistics are entirely environment dependent. As an example, to demonstrate the effectiveness of the analytical method, we assume $\eta(n)$ to be a correlated Gaussian random process with the following correlation function:

$$R_\eta(n_1, n_2) = \rho^{-|n_1-n_2|}.$$

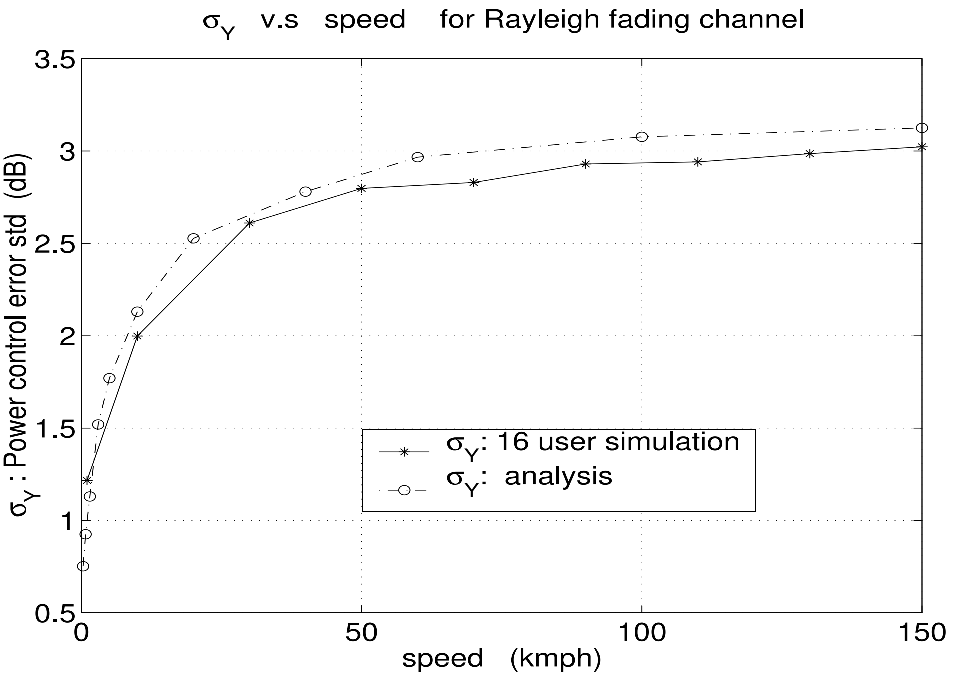

Figure 9: σ_Y v.s speed for one-path Rayleigh channel ($d = 0.5$ dB, $T = 1.25$ ms, $f_c = 900$MHz)

The state equation (18) is now given as:

$$X(n+1) = X(n) + d\Psi(B(n+1) - X(n)),$$

where

$$B(n+1) = -A(n) + I(n) + \Gamma^{tar}$$

We will again focus only on shadow fading for the desired user's signal. Thus the link gain $A(n)$ will be same as described in Section 3. However, because of the presence of external interference, the interference $I(n)$ is not a constant. Specifically, in the nth PCG, the interference is:

$$I(n) = 10 \log \frac{2\sum_{k=2}^{K} p_k^* + \eta^2(n) + N_0/2}{2}$$

We can use a similar method as in the case of Rayleigh fading to find the spectrum of $B(n)$. First, we generate the sequence of $B(n)$ by numerically generating the sequences of $A(n)$ and $\eta(n)$. Then, we can calculate the spectrum of $B(n)$ using standard spectrum estimation techniques [30]. Again, since the variation of η is slower compared with the power updates, we can still approximate the power control error Y to be Gaussian distributed. Thus for the variance σ_Y, the optimal K^* can still be found from equation (21). The power control error σ_Y^2 can then be calculated iteratively using equations (27) and (21).

In Figure 10, the mean of the other interference power is assumed to be 60% of total received signal power with an 8 dB variance. Its correlation coefficient $\rho = 0.5$. We assume there are 16 users in the system. Other parameters are set the same as in Figure 4. Note that in equation (14), both input A and total interference I are random processes. Simulation results are also plotted on the same figure. We can see that the analytical method in general works reasonably well.

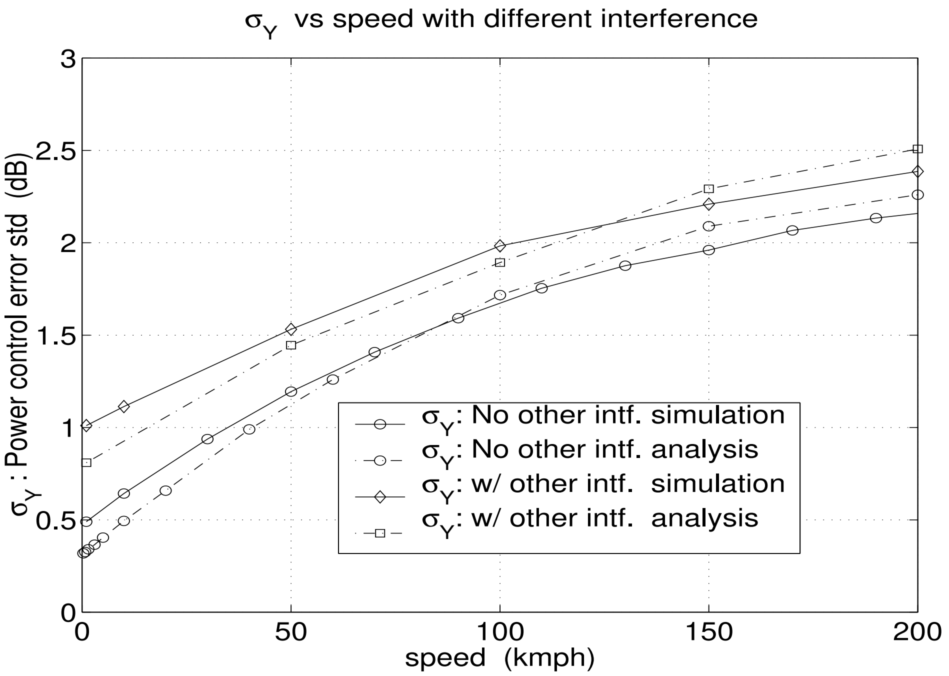

Figure 10: σ_Y v.s v ($d = 0.5$ dB, $D = 1$ m, $\xi = 0.1$, $T = 1.25$ ms, $\sigma_A = 3$ dB, $\rho = 0.5$.)

7 Conclusion

In this paper, a CDMA reverse link with the up/down algorithm power control was studied in the presence of fading. The effect of mobile speed, power control step size and fading channel parameters such as correlation coefficient and rate of fading on power control errors was investigated. First, we derived a stochastic nonlinear feedback control system model for the power controlled reverse link. And then, we studied the power control performance based on the nonlinear model using the technique of statistical linearization. Numerical results show excellent accuracy of our analysis. Such an analytical approach can be used to design and optimize the system parameters without going through lengthy simulations. For example, our analysis gives a direct method to evaluate power control stability and errors as a function of mobile speed, power control step size and fading channel parameters such as correlation coefficient and rate of fading. Such an approach is also useful in designing more advanced power control schemes such as in systems with multi-bit feedback or high order loop-filters. In this paper, the SIR measurement is assumed to be perfect and the effect of SIR measurement errors is a topic of further study.

References

[1] S. Grandhi, R. Vijayan, D. Goodman, and J. Zander, "Centralized Power Control in Cellular Radio Systems," *IEEE Trans. on Vehicular Technology*, vol. 42(4), pp. 466 – 468, 1993.

[2] J. Zander, "Performance of Optimum Transmitter Power Control in Cellular Radio Systems," *IEEE Trans. on Vehicular Technology*, vol. 41(1), pp. 57–62, 1992.

[3] R. Yates, "A Framework for Uplink Power Control in Cellular Radio System," *IEEE Journal on Selected Areas in Communications*, vol. 13(7), pp. 1341–1347, 1998.

[4] J. Zander, "Distributed Cochannel Interference Control in Cellular Radio Systems," *IEEE Trans. on Vehicular Technology*, vol. 41(1), pp. 305–311, 1992.

[5] G. Foschini and Z. Miljanic, "A Simple Distributed Power Autonomous Power Control Algorithm and its Convergence," *IEEE Trans. on Vehicular Technology*, vol. 42(4), pp. 641–646, 1994.

[6] S. Hanly and D. Tse, "Power control and capacity of spread-spectrum wireless networks," *Automatica*, vol. 35, pp. 1987 – 2012, Dec. 1999.

[7] TIA/EIA/IS-95, *Mobile Station-Base Station Compatibility for Dual-Mode Wideband Spread Spectrum Cellular System*, Telecommunication Industry Association, 1993.

[8] TIA/EIA/IS-95B, *Mobile Station-Base Station Compatibility for Dual-Mode Wideband Spread Spectrum Cellular System*, Telecommunication Industry Association, 1998.

[9] X. Z. Gao, J. M. A. Tanskanen, and S. J. Ovaska, "Power Control for Mobile DS/CDMA System Using a Modified MLMAN Neural Network Controller," in *Proc. IEEE Vehicular Technology Conference*, Phoenix, AZ, 1997, vol. 2, pp. 750 – 753.

[10] Q. Shen and W. Krzymien, "A Performance Improvement of Closed-Loop Power Control in CDMA Cellular Mobile Communication Systems," in *Proc. IEEE Vehicular Technology Conference*, Atlanta, GA, 1996, vol. 1, pp. 56 – 60.

[11] H. Su and E. Geraniotis, "Adaptive Closed-Loop Power Control with Quantized Feedback and Loop Filtering," in *Proc. IEEE International Symposium on Personal, Indoor and Mobile Radio Communications*, Boston, MA, 1998, vol. 1.

[12] J. Blom and F. Gunnarsson, *Power Control in Cellular Radio Systems*, Thesis No. 706, Department of Electrical Engineering, Linkopings Universitet, Linkopin, Sweden, 1998.

[13] L. Song, N. Mandayam, and Z. Gajic, "Analysis of an Up/Down Power Control Algorithm for CDMA Reverse Link: A Nonlinear Control System Approach," *CISS'99*, pp. 119 – 124, Mar. 1999.

[14] J. Herdtner and E. Chong, "Analysis of a Class of Asynchronous Power Control Algorithms for Cellular Wireless Systems," *IEEE Journal on Selected Areas in Communications*, vol. 18, pp. 436 – 446, March 2000.

[15] J. Holtzman, "A Simple, Accurate Method to Calculate SSMA Error Probability," *IEEE Trans. Communication*, vol. 49(3), pp. 461–464, March 1992.

[16] R. Morrow, "Accurate CDMA BER Calculation with Low Computational Complexity," in *IEEE Trans. on Communications*, November 1998, vol. 46(11), pp. 1114–1417.

[17] S. Ulukus and R. Yates, "Stochastic power control for cellular radio systems," *IEEE Transactions on Communication*, vol. 46, pp. 784–798, June. 1998.

[18] D. Ramakrishna, N. Mandayam, and R. Yates, "Subspace based estimation of the signal-to-interference ratio for cdma cellular," *IEEE Transactions on Vehicular Technology*, vol. 49, May 2000.

[19] Viterbi, *CDMA: Principles of Spread Spectrum Communications*, Addison-Wesley Publishing Company, 1995.

[20] A. Viterbi and R. Padovani, "Implication of Mobile Cellular CDMA," in *IEEE Communications Magazine*, December 1992, pp. 38–41.

[21] R. Padovani, "Reverse Link Performance of IS-95 Based Cellular Systems," in *IEEE Personal Communications Magazine*, 3rd Quarter 1994, vol. 1, pp. 28–34.

[22] G. Stuber, *Principles of Mobile Communication*, Kluwer Academic Publishers, 1996.

[23] M. Gudmundson, "Analysis of Handover Algorithm," in *VTC'91*, May 1991, vol. 1, pp. 537–541.

[24] M. Gudmundson, "Correlation Model for Shadow Fading in Mobile Radio Systems," *Electronics Letters*, vol. 27, pp. 2145–2146, November 1991.

[25] M. Dimentberg, *Statistical Dynamics of Nonlinear and Time Varying Systems*, John Wiley & Sons Inc., 1988.

[26] A. Fuller, *Nonlinear Stochastic Control Systems*, Barnes & Noble, New York, 1970.

[27] A. Pervozvanskii, *Random Process in Nonlinear Control System*, Academic Press, New York, 1965.

[28] Z. Gajic and M. Qureshi, *Lyapunov Matrix Equation in System Stability and Control*, Academic Press, San Diego, CA, 1995.

[29] Rec. ITU-R M.1225, *Guidelines for Evaluation of Radio Transmission Technologies for IMT-2000*, ITU, 1997.

[30] S. Kay, *Modern Spectral Estimation*, Prentice Hall, New York, 1993.

[31] W.C.Y. Lee, *Mobile Cellular Telecommunications: Analog and Digital Systems*, McGraw-Hill, New York, 1996.

[32] M. Yacoub, *Foundations of Mobile Radio Engineering*, CRC Press Inc., Boca Raton, Florida, 1993.